

Note added in proof.—Cross sections for ionization and excitation of Helium by protons to the levels $2p, k$, $3p, k$, $4p, k$, $3d, k$, and $4d, k$ have been calculated by A. Dalgarno and M. R. C. McDonald.¹⁵ Their

¹⁵ E. B. Armstrong and A. Dalgarno, *The Airglow and The Aurorae* (Pergamon Press, New York, 1955).

results differ considerably from the corresponding calculations of this paper. This is not surprising since the calculated cross-sections of this paper can vary from zero ($Z_3=1.6875$) to a maximum value for some choice of Z_3 . In conclusion the author expresses his gratitude to Professor A. Dalgarno for informing him of these calculations.

Hfs Anomaly of Sb^{121} and Sb^{123} Determined by the Electron Nuclear Double Resonance Technique

J. EISINGER AND G. FEHER

Bell Telephone Laboratories, Inc., Murray Hill, New Jersey

(Received July 16, 1957)

The ratios of the hyperfine interaction constants “ a ” and the nuclear g factors of the stable isotopes of antimony have been measured. From these measurements the hyperfine structure anomaly, defined as $\Delta = (a_{121}/a_{123})(g_{123}/g_{121}) - 1$, was found to be $(-0.352 \pm 0.005)\%$. Δ has its origin in the difference in the spatial distribution of the nuclear magnetic dipole for the two isotopes, which is related to the structure of the two nuclei. The experimental result is compared with theoretical values of Δ based on a variety of nuclear models.

The determination of a_{121}/a_{123} makes use of the electron nuclear double resonance (ENDOR) which is discussed in some detail. The sample used in the experiment was silicon doped with antimony and the microwave resonances were observed at ~ 9000 Mc/sec at a temperature of 1.2°K .

The ratio of the nuclear g factors was determined by conventional nuclear magnetic resonance techniques.

A. INTRODUCTION

THE hyperfine interaction constant a is a measure of the strength of the interaction between the nuclear magnetic dipole moment μ_I and the moment due to the orbital electron. For two isotopes (subscripts 1 and 2) of the same element in the same electronic state one might expect $(a_1/a_2) = (g_1/g_2)$, where we have written $g = \mu_I/I$.

By measuring the ratio of the interaction constants (e.g., by methods described in this paper or by atomic beams) and the ratio of the nuclear g factors (e.g., by nuclear magnetic resonance experiments) to high precision, deviations from this equality have been found.

It was pointed out by Kopfermann¹ and Bitter² that one should expect $(a_1/a_2) = (g_1/g_2)(1 + \Delta)$ for certain pairs of isotopes, where Δ is of the order of a fraction of one percent and is usually called the hyperfine structure (hfs) anomaly. Physically the origin of Δ can be traced to nuclear size effects, the most important of which is due to the difference in the distribution of the magnetic moment inside the nuclei under consideration.¹⁻³ A quantitative discussion of Δ from a theoretical point of view is left to a later section. Suffice it to say that such a calculation usually depends on the particular nuclear model chosen so that an experimental

determination of the hfs anomaly should be capable of adding to our knowledge of nuclear structure.

Hfs anomalies have been measured for several pairs of isotopes. Such experiments have been restricted until now to elements which lend themselves to detection in atomic beam experiments, i.e., mostly alkalis.^{2,4-7} Recent advances in the techniques of paramagnetic resonance experiments⁸ have made it possible to measure “ a ” with greater precision than had previously been possible. The method employed is called electron nuclear double resonance (ENDOR)⁸ and will be described in detail in a later section.

In the present experiment⁹ the precise ratio of the hyperfine interaction constants was determined by the ENDOR technique and the ratio of the nuclear g factor was redetermined by the NMR method for the two stable isotopes of antimony, Sb^{121} and Sb^{123} . The experimental value of Δ obtained in this manner was compared with values based on a variety of nuclear models.

B. ENERGY LEVELS AND TRANSITIONS

The magnetic interaction of an atom whose angular momentum $J = \frac{1}{2}$ and whose nucleus has a magnetic

⁴ Ochs, Logan, and Kusch, *Phys. Rev.* **78**, 184 (1950).

⁵ Eisinger, Bederson, and Feld, *Phys. Rev.* **86**, 73 (1952).

⁶ Jaccarino, Stroke, Edmonds, and Weiss, *Phys. Rev.* **105**, 590 (1957).

⁷ Y. Ting and H. Lew, *Phys. Rev.* **105**, 581 (1957).

⁸ G. Feher, *Phys. Rev.* **103**, 83 (1956).

⁹ A preliminary account of this work has been given [J. Eisinger and G. Feher, *Bull. Am. Phys. Soc. Ser. II*, **2**, 31 (1957)].

¹ H. Kopfermann, *Kernmomente* (Akademische Verlagsgesellschaft, Leipzig, 1940).

² F. Bitter, *Phys. Rev.* **76**, 150 (1949).

³ A. Bohr and V. F. Weisskopf, *Phys. Rev.* **77**, 94 (1950).

moment μ_I and spin I is given by the Hamiltonian

$$\mathcal{H} = a\mathbf{I} \cdot \mathbf{J} + g_J \mu_0 \mathbf{J} \cdot \mathbf{H} - g_I \mu_0 \mathbf{I} \cdot \mathbf{H}, \quad (1)$$

where H is the externally applied magnetic field, μ_0 is the Bohr magneton, and a is the hyperfine interaction constant which for a nuclear point dipole is given by the Fermi-Segrè formula^{10,11} (see below). The eigenvalues $W(F, m_F)$ of Eq. (1) are given by the Breit-Rabi equation,¹²

$$W(F, m_F) = -\frac{\Delta E}{2(I+1)} - g_I \mu_0 H m_F \pm \frac{\Delta E}{2} \left[1 + \frac{4m_F}{2I+1} x + x^2 \right]^{\frac{1}{2}}, \quad (2)$$

where $F = I \pm \frac{1}{2}$. The positive sign in the above expression corresponds to $I + \frac{1}{2}$ and the negative sign corresponds to $I - \frac{1}{2}$. $m_F = m_I \pm \frac{1}{2}$. The zero-field splitting $\Delta E = a(I + \frac{1}{2})$ and $x = (g_J + g_I)\mu_0 H / \Delta E = g_T \mu_0 H / \Delta E$, where g_J and g_I are the electronic and nuclear g factors.¹³

The energy level diagram for $I = \frac{5}{2}$ (corresponding to Sb¹²¹) is shown in Fig. 1. We show only the strong-field part of the diagram since in all of our experiments $x \geq 15$. The quantities that we need to determine in order to calculate the hyperfine structure anomaly are a , g_J , and g_I . We can observe experimentally two types

of transitions:

(a) $\Delta m_J = \pm 1$; $\Delta m_I = 0$ (i.e., $\Delta m_F = \pm 1$, $\Delta F = \pm 1$).

These are the microwave transitions that are observed in an ordinary paramagnetic resonance experiment and are labeled ν_e in Fig. 1. There are $2I+1$ such transitions. The unknown quantities are g_T and a , the experimentally determined quantities are ν_e and H . From Eq. (2) we obtain the expressions

$$a^2 \left[\frac{1}{4} \left(\frac{g_T \mu_0 H}{\nu_e + g_I \mu_0 H} \right)^2 - (I + \frac{1}{2})^2 \right] - a [2m_I g_T \mu_0 H] + (\nu_e + g_I \mu_0 H)^2 - (g_T \mu_0 H)^2 = 0, \quad (3)$$

$$g_T^2 \left[\left(\frac{\mu_0 H}{a} \right) - \frac{1}{4} \left(\frac{\mu_0 H}{\nu_e + g_I \mu_0 H} \right)^2 \right] + g_T 2m_I \left(\frac{\mu_0 H}{a} \right) + (I + \frac{1}{2})^2 - \left(\frac{\nu_e + g_I \mu_0 H}{a} \right)^2 = 0 \quad (4)$$

which are to be solved for a and g_T .

(b) $\Delta m_J = 0$, $\Delta m_I = \pm 1$ (i.e., $\Delta m_F = \pm 1$, $\Delta F = 0$).

These transitions occur at a much lower frequency than the microwave transitions and may be conveniently detected by the ENDOR technique.⁸ They are labeled ν_N^+ and ν_N^- in Fig. 1. As discussed in the next section they provide a more accurate way of determining a . From Eq. (2) we obtain

$$a^2 \left[\frac{1}{4} \left(\frac{g_T \mu_0 H}{\nu_N \pm g_I \mu_0 H} \right)^2 - (I + \frac{1}{2})^2 \right] - a [2m_I g_T \mu_0 H] + (\nu_N \pm g_I \mu_0 H)^2 - (g_T \mu_0 H)^2 = 0, \quad (5)$$

where the upper sign refers to the upper set of levels (i.e., $m_J = +\frac{1}{2}$) and the lower sign to the ($m_J = -\frac{1}{2}$) set. The absolute value of g_I is to be used in the above equation. However, for a positive g_I the m_I corresponding to the higher of the two levels, and for a negative g_I the m_I corresponding to the lower level, is to be taken.¹⁴

If one takes the difference between two transition frequencies which occur between levels of the same m_F 's, but different m_J , one can show from Eq. (2) that

$$\nu_N^+ - \nu_N^- = -2g_I \mu_0 H (m_F - m_F'). \quad (6)$$

Expression (6) provides a method for determining g_I . However, there are only $2I-1$ such "lucky" intervals. (See, for example the encircled ν_N in Fig. 1.) In order to minimize the experimental error it is desirable to make use of the $4I$ available pairs of transitions which occur between levels characterized by the same m_I

¹⁴ This enables one to determine signs of unknown moments, since a self-consistent set of a 's will be obtained only with a particular sign assignment.

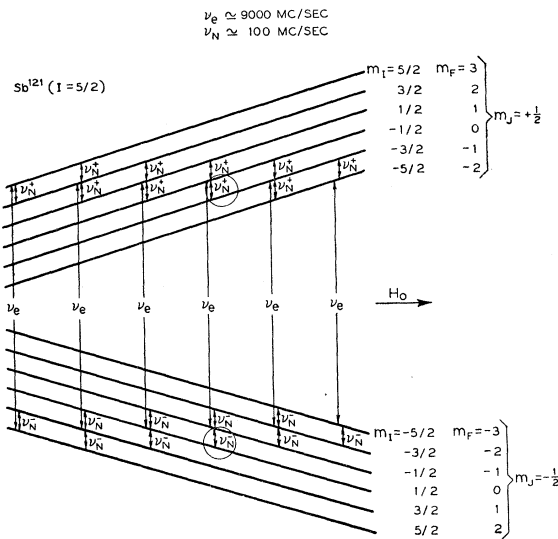


FIG. 1. Energy levels for Sb¹²¹ in Sb-doped Si in a high magnetic field. The electronic transitions ν_e and nuclear transitions ν_N^+ and ν_N^- observed in the experiment are indicated.

¹⁰ E. Fermi, Z. Physik **60**, 320 (1930).

¹¹ E. Fermi and E. G. Segrè, Z. Physik **82**, 729 (1933).

¹² G. Breit and I. I. Rabi, Phys. Rev. **38**, 2082 (1931).

¹³ The nuclear g factor g_I is defined as the ratio of the nuclear moment in Bohr magnetons to the nuclear spin. All other nuclear g factors (g , g_I , g_S , g_{exp} , etc.) which we will have occasion to use in later sections are understood to have units of nuclear magnetons divided by the appropriate spin quantum number, i.e., $g_I = (m/M)g$.

rather than m_F . Under those conditions an equation in g_I is found from Eq. (6):

$$\begin{aligned}
 &g_I^3(\mu_0 H)^3[4(\nu_{N^+} + \nu_{N^-})] \\
 &+ g_I^2(\mu_0 H)^2\{6[(\nu_{N^+})^2 - (\nu_{N^-})^2] - 2ag_T(\mu_0 H)\} \\
 &+ g_I(\mu_0 H)\{4[(\nu_{N^+})^3 + (\nu_{N^-})^3] - 4ag_T\mu_0 H[m_I\nu_{N^+} \\
 &+ (m_I - 1)\nu_{N^-}] - [2a^2(I + \frac{1}{2})^2 \\
 &+ 2(g_T\mu_0 H)^2](\nu_{N^+} + \nu_{N^-})\} + [(\nu_{N^+})^4 - (\nu_{N^-})^4] \\
 &- [a^2(I + \frac{1}{2})^2 + (g_T\mu_0 H)^2][(\nu_{N^+})^2 - (\nu_{N^-})^2] \\
 &- g_T a \mu_0 H[m_I(\nu_{N^+})^2 - (m_I - 1)(\nu_{N^-})^2] = 0, \quad (7)
 \end{aligned}$$

where as before for a positive g_I the m_I refers to the higher of the two upper levels and for a negative g_I to the lower of the two upper levels.

Since in our case $\nu_{N^-} - \nu_{N^+}$ is about an order of magnitude smaller than a , we cannot hope to get g_I to the same accuracy as a . For this reason the conventional NMR technique was used to obtain g_I to the desired accuracy. Equation (7) is presented for cases in which an NMR experiment is difficult to perform (e.g., radioactive nuclei or the nuclei of the rare-earth group). In order to evaluate g_I , g_T , and a from the above expressions one proceeds as follows: Eqs. (3) and (4) are solved for g_T and a , taking the published value of g_I . The value of g_T thus obtained is put into Eq. (5) which gives a more precise value of a . This new value may be substituted back into Eq. (4) to get an improved value of g_T . It should be noted, however, that only a small fraction of the inaccuracy in g_T is reflected in the final answer for a (the fraction being of the order $a/g_T\mu_0 H$; the same is true for an error in the determination of the magnetic field). If one is dealing with an unknown nuclear moment, Eq. (6) or (7) may be used to determine g_I .

The preceding discussion and some of the considerations to follow are more general than appears necessary for the experiment which is of immediate concern here, but since some of the experimental methods employed are novel a comprehensive discussion seems to be in order.

C. EXPERIMENTAL PROCEDURE

(a) Nuclear Spectrometer

The ratio of the nuclear moments of the Sb isotopes was determined with the aid of a commercial Varian V-4210A nuclear spectrometer.

The nuclear moments of Sb^{121} and Sb^{123} were reported by Proctor and Yu¹⁵ and Cohen *et al.*¹⁶ to an accuracy of 1 part in 10^4 . Since we are merely interested in the ratio of the moments, but this to a higher accuracy, we repeated the NMR experiments. The sample, similar to the one used by Proctor and Yu, was a solution of KSbF_6 in HF with approximately $0.1M$

of MnSO_4 .¹⁷ The dc magnetic field was kept constant and the rf frequency was varied. The resonance frequency corresponding to the center of the pattern was determined to 1 part in 10^5 . Since both nuclei see the same magnetic field, no corrections for shielding fields or chemical shifts need to be applied and the ratio of the resonance frequencies equals the ratio of the nuclear g -values.

(b) Microwave Spectrometer

The spectrometer used in this work operates at X-band ($\nu \approx 9000$ Mc/sec). It is a balanced-bridge type, so that the signal can be made proportional either to the real or imaginary part of the electronic susceptibility¹⁸ and it employs a superheterodyne detection scheme with an intermediate frequency of 60 Mc/sec. The magnetic field is modulated at 100 cps. A signal of this frequency is thus observed when passing through a resonance line and is detected by a phase-sensitive detector which follows the 100-cps audio amplifier. Its output has an integrating network which in all our experiments was adjusted to have a time constant of 0.25 sec. This output is fed directly into a recorder. In order to observe the microwave transitions the magnetic field is varied linearly and monitored by means of a nuclear probe, whose signal is superimposed on the electron resonance signal providing convenient field markers (see Fig. 2). The electron spin resonance frequency, the output of the nuclear probe and the frequency corresponding to the hyperfine transitions are all monitored by means of a frequency counter.

A rectangular cavity operating in the TE_{101} mode was used. It was made out of Pyrex and coated with silver on the inside. A slit was provided to allow the nuclear frequency, necessary for the ENDOR technique, to penetrate the cavity. This frequency was applied to a coil wrapped on the outside of the cavity which terminated in a 50-ohm transmission line. The cavity containing the sample was immersed in liquid helium at 1.2°K.

A more detailed description of the spectrometer is given elsewhere.¹⁹

(c) The Sample

The sample used was antimony-doped silicon. The paramagnetic resonance of such a sample was first observed by Fletcher *et al.*²⁰ Antimony is known to form a donor in silicon, four of its valence electrons forming covalent bonds with its neighboring silicon atoms and the fifth being bound to the Sb nucleus with

¹⁷ We are indebted to Dr. T. C. Loomis and Dr. R. G. Shulman for supplying the sample.

¹⁸ In view of the long relaxation times encountered, we were always tuned to the dispersion mode.

¹⁹ G. Feher, Bell System Tech. J. **26**, 449 (1957).

²⁰ Fletcher, Yager, Pearson, and Merritt, Phys. Rev. **95**, 844 (1954).

¹⁵ W. G. Proctor and F. C. Yu, Phys. Rev. **81**, 20 (1951).

¹⁶ Cohen, Knight, Wentink, and Koski, Phys. Rev. **79**, 191 (1950).

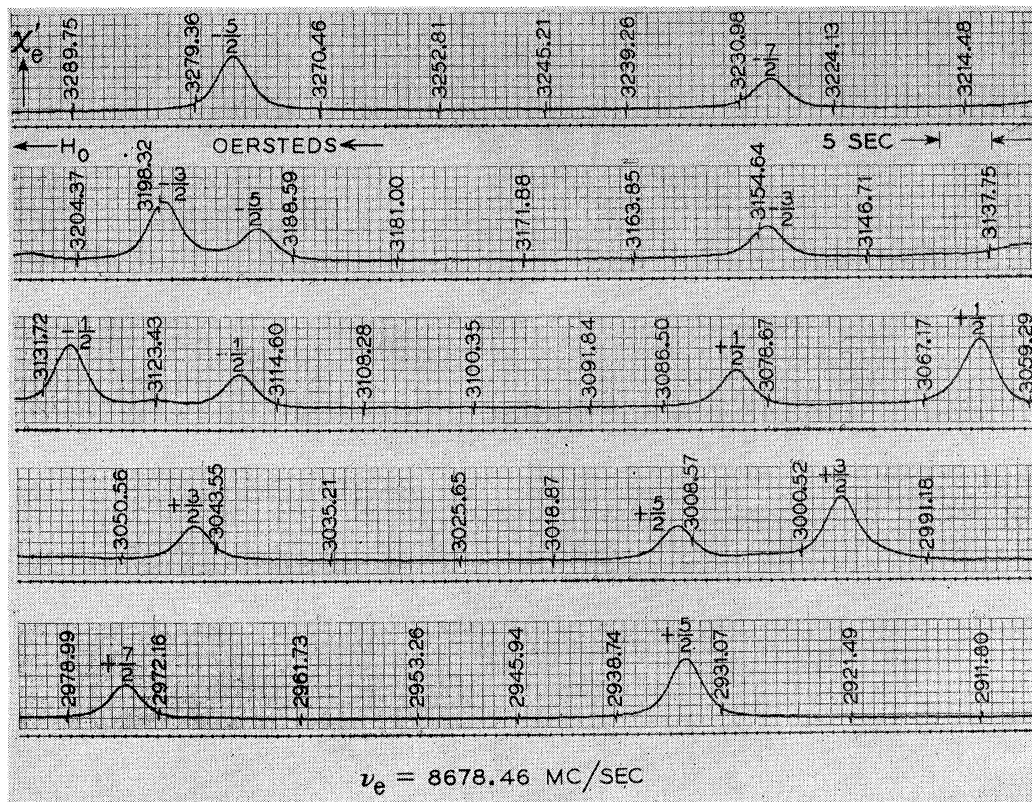


Fig. 2. Experimentally observed spectrum of the microwave transitions for Sb^{121} and Sb^{123} . The field markers are derived from a proton resonance.

an ionization energy of 0.039 eV.²¹ The wave function of this donor electron has been described in detail by Kohn and Luttinger.²² In order to obtain the maximum signal-to-noise ratio one would like to dope the silicon with as many antimony atoms as possible, the upper limit being given by undesired exchange effects arising from an overlap of the electronic wave functions.²³ These occur at a concentration of approximately 10^{17} atoms/cm³.²⁴ The sample that was used in our experiments had a room temperature resistivity of 0.17 ohm-cm corresponding to 5×10^{16} donors/cm³. Three pieces of silicon with dimensions $8 \times 12 \times 1$ mm were placed at the maximum microwave magnetic field region in the cavity. The low temperature of 1.2°K provided a convenient way of improving the signal-to-noise ratio by increasing the electronic Boltzmann factor. The electron spin lattice relaxation time at this temperature was of the order of a minute. Before each run the sample was allowed to come to thermal equilibrium at the desired magnetic field for at least 10 minutes.

²¹ Morin, Maita, Shulman, and Hannay, Phys. Rev. **96**, 833(A) (1954).

²² W. Kohn and J. M. Luttinger, Phys. Rev. **97**, 883 (1955).

²³ C. P. Slichter, Phys. Rev. **99**, 479 (1955).

²⁴ Feher, Fletcher, and Gere, Phys. Rev. **100**, 1784 (1955). Note that the figure captions in this reference should read 10^{17} donors per cm³ and 4×10^{17} donors per cm³.

(d) The ENDOR Technique

The principle of the electron nuclear double resonance (ENDOR) technique has been discussed earlier.⁸ It is based on the possibility of changing the population difference between two microwave levels (and hence the amplitude of the electron spin resonance signal) by inducing the hyperfine transition ν_N (see Fig. 1). A typical trace of the microwave resonance (dispersion) signal for Sb^{121} when the two transitions ($\frac{1}{2}, -\frac{5}{2} \leftrightarrow \frac{1}{2}, -\frac{3}{2}$) and ($-\frac{1}{2}, -\frac{5}{2} \leftrightarrow -\frac{1}{2}, -\frac{3}{2}$) are being induced is shown in Fig. 3. We note that (1) the second line traversed is approximately twice as large as the first and (2) the lines are highly asymmetrical, having a steep rise and a slower "decay." In order to understand the difference in amplitudes of the two lines we consider the population of the four levels which are involved in the transition under discussion as illustrated in Fig. 4. We make the following assumptions: (a) the electronic line can be completely saturated, (b) the hyperfine transitions ν_N are performed under fast adiabatic passage conditions²⁵ and therefore result in a complete reversal of the population, and (c) the only relaxation process by which thermal equilibrium is established involves $\Delta m_J = \pm 1$, $\Delta m_I = 0$ transitions.

²⁵ F. Bloch, Phys. Rev. **70**, 460 (1946).

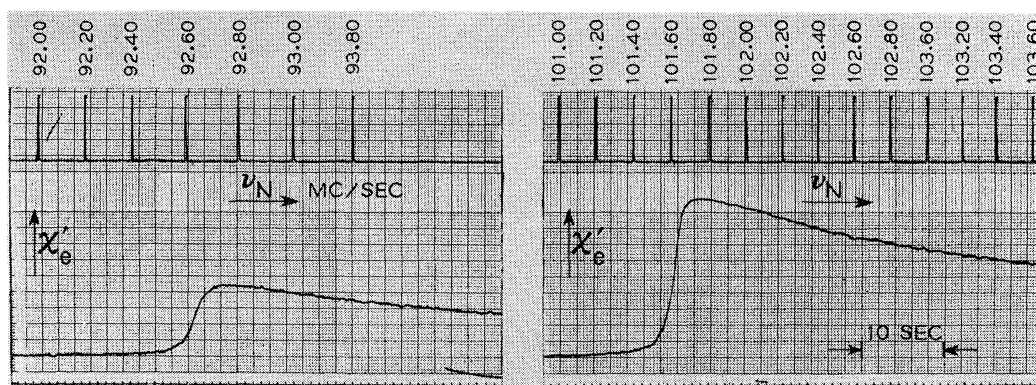


FIG. 3. Observation of the hyperfine transitions via the electron spin resonance line (ENDOR technique). The ratio of amplitudes is explained in Fig. 4. The asymmetry is caused by the long spin-lattice relaxation time [see Sec. C(d)].

Figure 4 shows the population of four levels during various stages of the ENDOR experiment. Figure 4(a) corresponds to thermal equilibrium, the lower states having a population of $N(1+\epsilon)$, where N is the total number of nuclei divided by the number of levels and 2ϵ is the electronic Boltzmann factor ($g_J\mu_0H/kT$). In Fig. 4(b) we saturate one of the electronic lines and thereby equalize the population of the levels involved in it. The amplitude of the electronic signal at this stage is very small (see Fig. 3). After inducing the ν_N^+ transitions we get a population difference between the two microwave levels of ϵ and the electron resonance signal will increase [see Fig. 4(c)]. After resaturating one electronic transition and waiting long enough for the other transition to come to thermal equilibrium, we arrive at the population as indicated in Fig. 4(d). After the ν_N^- transition is induced, the population is redistributed according to Fig. 4(e). We now see that the population difference between the two microwave levels is 2ϵ . This means that the second signal is expected to be twice as large as the first. This corresponds approximately to the experimentally found ratio as can be seen from Fig. 3. If one induces the ν_N^- and then the ν_N^+ transition one would expect by a similar analysis a symmetric situation, i.e., the second line should again be twice as large as the first. Experimentally we find a small asymmetry in the ratio of the amplitudes depending on the direction of the nuclear frequency sweep. This can be traced to a breakdown of our assumption that the relaxation proceeds only via $\Delta m_J = \pm 1$, $\Delta m_I = 0$ transitions. If we have a simultaneous electron-nuclear flip (i.e., $\Delta m_J = \pm 1$, $\Delta m_I = \mp 1$) we would not expect a symmetrical situation.²⁶ If this "cross relaxation" is the predominant process and one does not wait long enough for the $\Delta m_J = \pm 1$ relaxation process to establish thermal equilibrium, one can show for our case that the expected ratio of amplitudes should

²⁶ This asymmetry will be different for positive and negative moments and may be used therefore to determine the sign of unknown moments. The asymmetry is also helpful in determining the various relaxation times.

be 3:2 and 3:1 depending on the direction of the sweep. The magnitude of the cross relaxation time was calculated by Pines, Bardeen, and Slichter²⁷ to be 40–100 minutes and is therefore expected to affect the symmetry only to a small extent.²⁸

The assumption of complete saturation is also an oversimplification. If one deals with an inhomogeneously broadened line²⁹ and uses magnetic-field modulation which sweeps over a fraction of the line under fast adiabatic passage conditions one can show that only the portion of the line corresponding to the center of the field sweep should be completely saturated. The rest of the line covered by the sweep has different degrees of saturation. The portion near the extremes of the sweep are not saturated at all.

The assumption of inducing the hyperfine transitions under fast adiabatic passage conditions is in our experiments easily satisfied although it should be noted that this is not a necessity for the ENDOR technique to work. For instance, a saturation of the hyperfine transition would be sufficient. It would merely reduce the observed signal by a factor of two.

The asymmetry of the line arises from the fact that it takes a time of the order of a relaxation time to resaturate the electronic resonance line. This is responsible for the slow trailing off of the signal. The steeper rise during the first half of the traversal through the line is given by the inherent line width of the hf transition.

D. EXPERIMENTAL RESULTS

(a) Nuclear Resonance Transition

We find for the ratio of the nuclear resonance frequencies of Sb^{121} and Sb^{123} ,

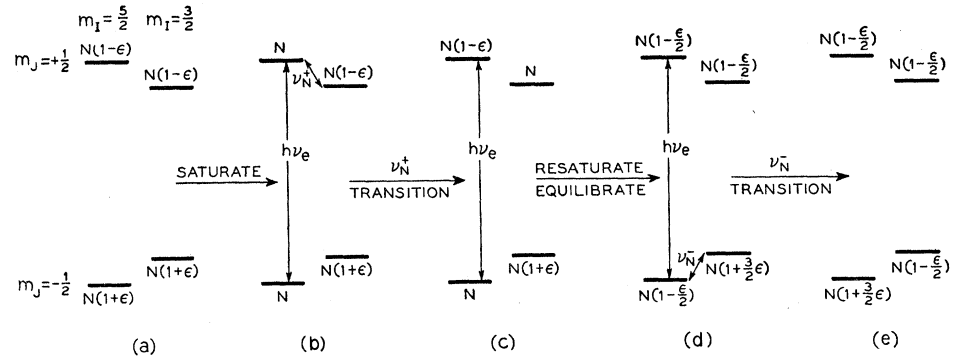
$$\nu_{121}/\nu_{123} = g_{121}/g_{123} = 1.84661 \pm 0.00001. \quad (8)$$

²⁷ Pines, Bardeen, and Slichter, Phys. Rev. **106**, 489 (1957).

²⁸ In a high-concentration sample where exchange effects become important, a different cross relaxation mechanism takes place which also permits the determination of the sign of the magnetic moment [see Feher, Fuller, and Gere, Phys. Rev. **107**, 1462 (1957)].

²⁹ A. M. Portis, Phys. Rev. **103**, 834 (1956).

FIG. 4. Population of the four levels which are responsible for the resonance spectrum of Fig. 3. Note that after the first hyperfine transition the population difference of the microwave levels is ϵ [see 4(c)] and after the second transition it is 2ϵ [see 4(d)]. This accounts for the second signal being larger than the first (see Fig. 3). 2ϵ =electronic Boltzmann factor $g_J\mu_0H/kT$; N =total number of spins divided by the number of energy levels.



This is in agreement with previous determinations^{15,16} within their experimental errors.

(b) Microwave Transitions

Figure 2 shows the paramagnetic resonance lines with a linearly varying magnetic field. We see six lines due to the Sb¹²¹ ($I=5/2$) and eight lines due to Sb¹²³ ($I=7/2$). In addition small background lines are observed, whose position correspond to arsenic and phosphorus which were accidental trace impurities in the sample. The lines are inhomogeneously broadened²⁹ and have a shape similar to the dispersion under adiabatic fast passage conditions.²⁵ A more detailed discussion of the line shape will be published later. The magnetic field markers which are superimposed on the trace are derived from the proton signal and have the usual characteristic shape of the derivative of an absorption.

In order to improve the statistics, we made four pairs of runs similar to the one shown in Fig. 2. Each pair consisted of one run with increasing magnetic field and one with decreasing magnetic field. The results are summarized in Table I. From the above data we find, with the aid of Eq. (4),

$$g_J = 1.99853 \pm 0.00001. \tag{9}$$

The error in (9) is the most probable error obtained from the spread of data given in Table I. The error in

TABLE I. Magnetic fields at which the microwave resonances occur. The listed values are averages of 8 runs. From the above data one can obtain g_J and the hyperfine interaction constant "a". The latter may be obtained more accurately from the data in Table II.

Sb ¹²³			Sb ¹²¹		
H oersteds	Transition m_J	g_J	H oersteds	Transition m_J	g_J
2974.63	1/2 to 3/2	1.99857	2933.63	1/2 to 3/2	1.99856
3009.63		1.99858			2997.48
3045.13	-1/2 to -3/2	1.99854	3062.99	-1/2 to -3/2	1.99849
3081.04		1.99851			3129.71
3117.28	-3/2 to -1/2	1.99854	3197.92	-3/2 to -1/2	1.99854
3154.02		1.99853			3267.65
3191.21	-5/2 to -3/2	1.99848			
3228.75		1.99851			

$\nu_e = 8678.46$ Mc/sec Average $g_J = 1.99853 \pm 0.00001$

the absolute value of g_J may however be somewhat larger due to the field differences between the positions of the nuclear probe and the paramagnetic sample which may amount to as much as ± 30 milli-oersteds depending on the cycling procedure used in establishing the magnetic field. This may result in a systematic error in the g -determination of 2 parts in 10^5 .

In any event the accuracy of the final result will not be affected by the error in g_J since it enters only through correction terms arising from the fact that we are not quite in the Paschen-Back field region.

From the data of Table I one can, with the aid of Eq. (3), calculate the following values of a :

$$\begin{aligned} a_{121} &= 186.80 \pm 0.04 \text{ Mc/sec,} \\ a_{123} &= 101.51 \pm 0.02 \text{ Mc/sec.} \end{aligned} \tag{10}$$

The values given in (10) lead to a value of the hfs anomaly $\Delta = \epsilon_{121} - \epsilon_{123} = -(0.35 \pm 0.03)\%$. In order to improve this accuracy we resorted to the double resonance technique as discussed before.

(c) The ENDOR Transitions

The asymmetric shape of the signal obtained when sweeping through ν_N (see Fig. 3) was discussed in a previous section. The frequency determinations were made at half the height of the steeply rising part. Two such determinations were made for each transition; one with the rf field varying from low to high frequencies and the other from high to low frequencies. The difference between the two frequency determinations corresponds approximately to the nuclear line width and was found to be about two orders of magnitude smaller than the width of the microwave transition. This reduction in line width is possible because of the inhomogeneous broadening²⁹ of the electron spin resonance line and is the basis of the higher accuracy attainable by the ENDOR technique. The average of the two readings was taken as the center of the resonance line and corresponds to the hyperfine transition frequency tabulated in Table II, together with the transitions involved, the magnetic field strengths and the microwave frequency. From the tabulated data we obtain, with the aid of Eq. (5), for the hyperfine structure

TABLE II. Determination of the hyperfine interaction constant "a" for Sb¹²¹ and Sb¹²³ by the ENDOR technique. The values for "a" are obtained from the above data by means of Eq. 5.

Saturated electronic transition $m_I, m_I \leftrightarrow m_I, m_I$	ν_e (Mc/sec)	H (oersteds)	Hyperfine transitions $m_I, m_I \leftrightarrow m_I, m_I$	ν_N (Mc/sec)	a (Mc/sec)				
$\frac{1}{2}, \frac{5}{2} \leftrightarrow -\frac{1}{2}, \frac{5}{2}$	906 6.3	3072.1	Sb ¹²¹	$\frac{1}{2}, \frac{5}{2} \leftrightarrow -\frac{1}{2}, \frac{5}{2}$	93.457	186.809			
				$-\frac{1}{2}, \frac{5}{2} \leftrightarrow -\frac{1}{2}, \frac{5}{2}$	85.402	186.784			
				$\frac{1}{2}, \frac{3}{2} \leftrightarrow -\frac{1}{2}, \frac{3}{2}$	85.441	186.805			
				$-\frac{1}{2}, \frac{3}{2} \leftrightarrow -\frac{1}{2}, \frac{3}{2}$	93.583	186.803			
				$\frac{1}{2}, \frac{1}{2} \leftrightarrow -\frac{1}{2}, \frac{1}{2}$	87.190	186.803			
				$-\frac{1}{2}, \frac{1}{2} \leftrightarrow -\frac{1}{2}, \frac{1}{2}$	95.434	186.789			
				$\frac{1}{2}, \frac{3}{2} \leftrightarrow -\frac{1}{2}, \frac{1}{2}$	87.190	186.812			
				$-\frac{1}{2}, \frac{3}{2} \leftrightarrow -\frac{1}{2}, \frac{1}{2}$	95.523	186.791			
				$\frac{1}{2}, \frac{1}{2} \leftrightarrow -\frac{1}{2}, -\frac{1}{2}$	89.004	186.791			
				$-\frac{1}{2}, \frac{1}{2} \leftrightarrow -\frac{1}{2}, -\frac{1}{2}$	97.464	186.795			
				$\frac{1}{2}, -\frac{1}{2} \leftrightarrow -\frac{1}{2}, -\frac{1}{2}$	904 5.7	3261.2	$\frac{1}{2}, \frac{1}{2} \leftrightarrow -\frac{1}{2}, -\frac{1}{2}$	88.973	186.808
							$-\frac{1}{2}, -\frac{1}{2} \leftrightarrow -\frac{1}{2}, -\frac{1}{2}$	97.522	186.808
			$\frac{1}{2}, -\frac{1}{2} \leftrightarrow -\frac{1}{2}, -\frac{1}{2}$	90.868	186.794				
			$-\frac{1}{2}, -\frac{1}{2} \leftrightarrow -\frac{1}{2}, -\frac{1}{2}$	99.547	186.807				
$\frac{1}{2}, -\frac{3}{2} \leftrightarrow -\frac{1}{2}, -\frac{3}{2}$	904 4.5	3328.8	Sb ¹²¹	$\frac{1}{2}, -\frac{3}{2} \leftrightarrow -\frac{1}{2}, -\frac{3}{2}$	90.791	186.804			
				$-\frac{1}{2}, -\frac{3}{2} \leftrightarrow -\frac{1}{2}, -\frac{3}{2}$	99.561	186.809			
				$\frac{1}{2}, -\frac{1}{2} \leftrightarrow -\frac{1}{2}, -\frac{3}{2}$	92.779	186.816			
				$-\frac{1}{2}, -\frac{1}{2} \leftrightarrow -\frac{1}{2}, -\frac{3}{2}$	101.668	186.799			
$\frac{1}{2}, -\frac{5}{2} \leftrightarrow -\frac{1}{2}, -\frac{5}{2}$	904 2.3	3397.5	Sb ¹²¹	$\frac{1}{2}, -\frac{5}{2} \leftrightarrow -\frac{1}{2}, -\frac{5}{2}$	92.646	186.800			
				$-\frac{1}{2}, -\frac{5}{2} \leftrightarrow -\frac{1}{2}, -\frac{5}{2}$	101.639	186.806			
			Average value		186.802±0.005				
$\frac{1}{2}, \frac{7}{2} \leftrightarrow -\frac{1}{2}, \frac{7}{2}$	906 6.3	3113.2	Sb ¹²³	$\frac{1}{2}, \frac{7}{2} \leftrightarrow -\frac{1}{2}, \frac{7}{2}$	47.034	101.506			
				$-\frac{1}{2}, \frac{7}{2} \leftrightarrow -\frac{1}{2}, \frac{7}{2}$	51.010	101.515			
				$\frac{1}{2}, \frac{5}{2} \leftrightarrow -\frac{1}{2}, \frac{5}{2}$	47.042	101.520			
				$-\frac{1}{2}, \frac{5}{2} \leftrightarrow -\frac{1}{2}, \frac{5}{2}$	51.040	101.529			
				$\frac{1}{2}, \frac{3}{2} \leftrightarrow -\frac{1}{2}, \frac{3}{2}$	47.566	101.509			
				$-\frac{1}{2}, \frac{3}{2} \leftrightarrow -\frac{1}{2}, \frac{3}{2}$	51.584	101.522			
				$\frac{1}{2}, \frac{1}{2} \leftrightarrow -\frac{1}{2}, \frac{3}{2}$	47.565	101.516			
				$-\frac{1}{2}, \frac{1}{2} \leftrightarrow -\frac{1}{2}, \frac{3}{2}$	51.614	101.508			
				$\frac{1}{2}, \frac{3}{2} \leftrightarrow -\frac{1}{2}, \frac{1}{2}$	48.106	101.517			
				$-\frac{1}{2}, \frac{3}{2} \leftrightarrow -\frac{1}{2}, \frac{1}{2}$	52.170	101.504			
				$\frac{1}{2}, \frac{1}{2} \leftrightarrow -\frac{1}{2}, \frac{1}{2}$	904 7.0	3213.7	$\frac{1}{2}, \frac{1}{2} \leftrightarrow -\frac{1}{2}, \frac{1}{2}$	48.096	101.515
							$-\frac{1}{2}, \frac{1}{2} \leftrightarrow -\frac{1}{2}, \frac{1}{2}$	52.196	101.512
			$\frac{1}{2}, \frac{3}{2} \leftrightarrow -\frac{1}{2}, \frac{1}{2}$	48.644	101.505				
			$-\frac{1}{2}, \frac{3}{2} \leftrightarrow -\frac{1}{2}, \frac{1}{2}$	52.774	101.525				
$\frac{1}{2}, -\frac{1}{2} \leftrightarrow -\frac{1}{2}, -\frac{1}{2}$	904 7.0	3249.1	Sb ¹²³	$\frac{1}{2}, -\frac{1}{2} \leftrightarrow -\frac{1}{2}, -\frac{1}{2}$	48.633	101.515			
				$-\frac{1}{2}, -\frac{1}{2} \leftrightarrow -\frac{1}{2}, -\frac{1}{2}$	52.789	101.519			
				$\frac{1}{2}, \frac{1}{2} \leftrightarrow -\frac{1}{2}, -\frac{1}{2}$	49.202	101.523			
				$-\frac{1}{2}, \frac{1}{2} \leftrightarrow -\frac{1}{2}, -\frac{1}{2}$	53.336	101.504			
$\frac{1}{2}, -\frac{3}{2} \leftrightarrow -\frac{1}{2}, -\frac{3}{2}$	904 5.7	3285.5	Sb ¹²³	$\frac{1}{2}, -\frac{3}{2} \leftrightarrow -\frac{1}{2}, -\frac{3}{2}$	49.178	101.519			
				$-\frac{1}{2}, -\frac{3}{2} \leftrightarrow -\frac{1}{2}, -\frac{3}{2}$	53.384	101.517			
				$\frac{1}{2}, -\frac{1}{2} \leftrightarrow -\frac{1}{2}, -\frac{3}{2}$	49.756	101.519			
				$-\frac{1}{2}, -\frac{1}{2} \leftrightarrow -\frac{1}{2}, -\frac{3}{2}$	53.982	101.516			
$\frac{1}{2}, -\frac{5}{2} \leftrightarrow -\frac{1}{2}, -\frac{5}{2}$	904 4.5	3322.1	Sb ¹²³	$\frac{1}{2}, -\frac{5}{2} \leftrightarrow -\frac{1}{2}, -\frac{5}{2}$	49.730	101.524			
				$-\frac{1}{2}, -\frac{5}{2} \leftrightarrow -\frac{1}{2}, -\frac{5}{2}$	53.990	101.523			
				$\frac{1}{2}, -\frac{3}{2} \leftrightarrow -\frac{1}{2}, -\frac{5}{2}$	50.319	101.520			
				$-\frac{1}{2}, -\frac{3}{2} \leftrightarrow -\frac{1}{2}, -\frac{5}{2}$	54.598	101.515			
$\frac{1}{2}, -\frac{7}{2} \leftrightarrow -\frac{1}{2}, -\frac{7}{2}$	904 3.1	3358.9	Sb ¹²³	$\frac{1}{2}, -\frac{7}{2} \leftrightarrow -\frac{1}{2}, -\frac{7}{2}$	50.284	101.521			
				$-\frac{1}{2}, -\frac{7}{2} \leftrightarrow -\frac{1}{2}, -\frac{7}{2}$	54.598	101.520			
			Average value		101.516±0.004				

constants,

$$a_{121} = 186.802 \pm 0.005 \text{ Mc/sec}, \quad (11)$$

$$a_{123} = 101.516 \pm 0.004 \text{ Mc/sec},$$

$$a_{121}/a_{123} = 1.84012 \pm 0.00009. \quad (12)$$

From (8) and (12) we finally obtain, for the hfs anomaly,

$$\Delta = \frac{a_{121} g_{123}}{a_{123} g_{121}} - 1 = -(0.352 \pm 0.005)\%. \quad (13)$$

The nuclear g values may be obtained with the aid of Eq. (7). The values including a diamagnetic correction³⁰ of 0.52% are

$$\begin{aligned} g(\text{Sb}^{121}) &= 1.3440 \pm 0.0006, \\ g(\text{Sb}^{123}) &= 0.7281 \pm 0.0003. \end{aligned} \quad (14)$$

The values in (14) agree with the previously published values.^{15,16} As mentioned earlier we used the more precisely determined ratio of g values (8) in the determination of Δ . The results in (14) are merely quoted to illustrate the use of the ENDOR technique in determining nuclear g values.

E. THEORETICAL CONSIDERATIONS

The magnetic interaction is given by the Hamiltonian of Eq. (1). The hyperfine structure constant " a " has been calculated by Fermi and Segre^{10,11} with the assumption that the nucleus is infinitesimally small and its moment a point dipole. They obtain

$$ha_{pd} = \frac{16\pi}{3} \frac{\mu_N}{\mu_0} |\psi(0)|^2, \quad (15)$$

where $\psi(0)$ is the electronic wave function at the nucleus.

If we allow the nucleus to have a finite extent, we must modify (15) by taking the electronic wave function and the distribution of the magnetic moment inside the nucleus into account. Expression (15) may then be rewritten

$$ha = \frac{16\pi}{3} \frac{\mu_N}{\mu_0} |\psi(0)|^2 (1 + \epsilon^{\text{BW}})(1 + \epsilon^{\text{RB}}). \quad (16)$$

The factor $(1 + \epsilon^{\text{BW}})$ takes into account the so-called Bohr-Weisskopf³ effect which has its origin in the distribution of the nuclear magnetic moment and whose existence was suggested by Kopfermann¹ and Bitter² before being calculated by Bohr and Weisskopf. The factor $(1 + \epsilon^{\text{RB}})$ is due to the Rosenthal-Breit³¹⁻³³ effect which is caused by the electron moving in a Coulomb field modified by the finite size of the nucleus. It follows from equation (16) that, if we are dealing with two isotopes of the same element identified by the subscripts 1 and 2, then

$$(a_1/a_2) = (g_1/g_2)(1 + \Delta^{\text{BW}} + \Delta^{\text{RB}}), \quad (17)$$

where $\Delta \simeq \epsilon_1 - \epsilon_2$ and where we have assumed that the electronic wave functions at the nucleus are the same for both isotopes. In the following sections we shall attempt to calculate Δ^{BW} and Δ^{RB} for the two stable antimony isotopes and compare our results with the experimental value of Δ .

(a) Rosenthal-Breit Effect

Owing to the finite size of the nucleus the potential field in which the orbital electron moves is cut off at the nuclear boundary. This results in a lower value of the electronic wave function ψ than would obtain for a point nucleus so that ϵ^{RB} will always be negative. A method for calculating this effect is given by Crawford and Schawlow.³⁴ One obtains for Sb¹²¹ a value for ϵ^{RB} of 2×10^{-2} . In order to calculate $\Delta^{\text{RB}} = \epsilon^{\text{RB}}(\text{Sb}^{121}) - \epsilon^{\text{RB}}(\text{Sb}^{123})$ one has to know the change in nuclear radius, δR , in going from Sb¹²¹ to Sb¹²³. This may be estimated from a semiempirical relationship based on a compressible model of the nucleus and discussed by Wilets, Hill, and Ford.³⁵ In this way we find $(\delta R/R_0) = -4 \times 10^{-3}$ which leads to a value of $\Delta^{\text{RB}} = -8 \times 10^{-5}$. This effect is many times smaller than the Bohr-Weisskopf effect discussed in the following section.

(b) Bohr-Weisskopf Effect

The effect of the finite extent of the nuclear moment was considered by Bohr and Weisskopf³ for a spherically symmetrical magnetic moment distribution taking into account the variation of the radial electron wave function inside a uniformly charged nucleus. The nuclear moment is made up of a contribution due to spin and one due to orbital moment. These have essentially different spatial distribution and therefore need to be considered separately. Bohr and Weisskopf find

$$\epsilon^{\text{BW}} = -(\alpha_s + 0.62\alpha_l)b(R^2/R_0^2)_{Av}, \quad (18)$$

where α_s and α_l are the fractions of the magnetic moment due to spin and orbital angular momentum, respectively, and b is a parameter which depends on Z and R_0 , the nuclear radius. It is 1.17% for antimony. $(R^2/R_0^2)_{Av}$ describes the mean radius of the portion of the nucleus which contributes to the magnetic moment. R is therefore a sort of mean magnetic moment radius.

Bohr^{36,37} refined these calculations by taking into account the angular asymmetry of the spin distribution which may have a considerable effect on the hfs anomaly. He obtains

$$\epsilon^{\text{BW}} = -[(1 + 0.38\zeta)\alpha_s + 0.62\alpha_l]b(R^2/R_0^2)_{Av}, \quad (19)$$

where $\zeta = 0$ for the uniform model of the nucleus but ζ differs from zero for the single-particle and collective models. Its value depends on the particular model chosen and is discussed by Bohr.³⁷

(c) Consideration of Solid-State Effects on the hfs Anomaly

All previous theoretical and experimental work on the hyperfine structure anomaly was performed on

³⁰ W. E. Lamb, Jr., Phys. Rev. **60**, 817 (1941).

³¹ J. E. Rosenthal and G. Breit, Phys. Rev. **41**, 459 (1932).

³² G. Breit, Phys. Rev. **42**, 348 (1932).

³³ G. Racah, Nature **129**, 723 (1932).

³⁴ M. F. Crawford and A. L. Schawlow, Phys. Rev. **76**, 1310 (1949).

³⁵ Wilets, Hill, and Ford, Phys. Rev. **91**, 1488 (1953).

³⁶ A. Bohr, Phys. Rev. **81**, 134 (1951).

³⁷ A. Bohr, Phys. Rev. **81**, 331 (1951).

isolated atomic systems. In this section we wish to explore whether any of the relations [e.g., Eqs. (17), (18), and (19)] have to be modified in the solid and whether any interaction peculiar to the solid have to be taken into account.

The wave function of the donor electron in silicon has been calculated in detail by Kohn and Luttinger.²² They find a wave function of the form

$$\psi(\mathbf{r}) = \sum_{i=1}^N F_i(\mathbf{r}) \varphi_i(\mathbf{r}),$$

where N is the number of equivalent minima (the conduction band in silicon having 6 minima along the [100] direction), $\varphi_i(\mathbf{r})$ is the Bloch wave at the i th minimum, and $F_i(\mathbf{r})$ is the envelope wave function obtained by solving an effective mass Schrödinger equation. It resembles a hydrogenic s state having a much larger effective radius because of the high dielectric constant of silicon. This is also the main reason why the hyperfine interaction in the solid is much smaller than in the corresponding atomic case. However, in the hfs anomaly the magnitude of this interaction is not important since only the ratio of the interactions enters the calculation. Also the detailed behavior of the electron outside the nucleus will be of little importance since the hyperfine interaction arises essentially when the electron is inside the nucleus and its behavior there will be the same whether one deals with an isolated atom or an atom imbedded in a solid. (This is evident from the fact that the ionization energy which is characteristic of the behavior of the electron outside the nucleus is many orders of magnitudes smaller than the energy of the electron inside the nucleus.)

An effect that could perturb the observed hf splitting arises from an interaction of the nuclear quadrupole moment with electric field gradients in the crystal. Although the tetrahedral symmetry of the donors in silicon precludes a quadrupole interaction, a strain in the crystal would destroy this symmetry and thereby produce an electric field gradient at the donor site. However, since the magnitude of the quadrupole interaction depends on m_I , the measured hf splittings should be different according to the m_I levels involved. From Table II we see that such a variation was not found experimentally. From this we conclude that quadrupole effects if any were negligibly small in our experiment.³⁸

Another effect which has to be considered is that due to zero-point lattice vibrations. In order to make a rough estimate of this effect we assume that the electron can follow the motion of the nucleus. The

³⁸ It would be instructive from a solid-state point of view to apply an external force and measure by the ENDOR technique the electric field gradients produced. Experiments along similar lines were performed by Shulman, Wyluda, and Anderson [Phys. Rev. **107**, 953 (1957)] using standard nuclear resonance techniques. Their method, however, is not applicable to donors in silicon.

change in the electronic wave function will then be given approximately by

$$|\Delta\psi(0)|^2/|\psi(0)|^2 \simeq (x/a)^2,$$

where a is the donor-silicon distance (2.5×10^{-8} cm) and x is the amplitude of the zero-point vibrations ($\sim 10^{-9}$ cm) which causes the distortion of the wave functions. We are only concerned with the difference of this effect for the two isotopes having masses M_1 and M_2 which will be $1 - (M_1/M_2)^{3/2} \simeq 10^{-2}$ of the total effect. From this estimate we find that the measured hfs anomaly may be numerically too large by about 2 parts in 10^5 . Since in our case this is smaller than the quoted experimental error, the effect was neglected in the analysis of the data. For nuclei with lighter masses this effect will of course be larger and for the H^1 , H^2 pair may become a fraction of a percent, exceeding the hfs anomaly as measured on atomic systems by an order of magnitude.

(d) Description of Nuclear Models

The hfs anomaly is one of several nuclear parameters which can be measured and calculated on the basis of different nuclear models,³⁹ so that it may hopefully contribute to the understanding of the structure of various nuclei. In what follows, we shall discuss the two antimony isotopes Sb^{121} and Sb^{123} in the light of four models: the extreme single-particle model (SP), the collective model (C), one that we might call the configuration mixing model (CM), and the single-particle—uniform-interpolation model (SU).

I. Extreme Single-Particle Model (SP)

This is the simplest model and forms the basis of the more sophisticated models discussed below.

The two Sb isotopes contain an even number of neutrons (70 and 72) which are assumed to form a closed shell with no net angular momentum, and 51 protons, 50 of which form a nuclear core along with the neutrons, leaving one proton to describe an orbit about the core. The odd proton is thought to be the sole contributor to the spin, moment, quadrupole moment, and hfs anomaly of the nucleus. In view of the fact that 50 is a magic number, the SP model can be expected to be well adapted to Sb. The state of the odd proton is obtained from the known spin and the systematics of the available energy levels⁴⁰ and is $d_{3/2}$ and $g_{7/2}$ for Sb^{121} and Sb^{123} , respectively.

It is readily seen that the magnetic moment is given by

$$g = \frac{\mathbf{S} \cdot \mathbf{I}}{I(I+1)} g_s + \frac{\mathbf{L} \cdot \mathbf{I}}{I(I+1)} g_l,$$

³⁹ Many of the models discussed below are reviewed in R. J. Blin-Stoyle, *Revs. Modern Phys.* **28**, 92 (1956).

⁴⁰ M. G. Mayer, *Phys. Rev.* **78**, 16 (1950); Haxel, Jensen, and Suess, *Naturwissenschaften* **35**, 375 (1948); L. A. Nordheim, *Revs. Modern Phys.* **23**, 322 (1951).

from which

$$\mu_{\text{SP}} = I g = I [g_l \pm (g_s - g_l) / (2l + 1)]; \quad I = l \pm \frac{1}{2}, \quad (20)$$

where l is the orbital angular momentum quantum number of the odd particle and g_s and g_l are its spin and orbital g factors, respectively; $g_s = 5.585$ and -3.826 and $g_l = 1$ and 0 for protons and neutrons, respectively. The values of μ_{SP} calculated in this way are only within some 40% of the experimental values, μ_{exp} , and are given in Table III. They are the well-known Schmidt values.⁴¹

In order to calculate a value for the hfs anomaly, we must estimate the contributions of spin and orbital moment, α_s and α_l . Using (19) and (20), we find that

$$\begin{aligned} \alpha_s &= (\mathbf{S} \cdot \mathbf{I}) g_s / [I(I+1)g] \\ &= \pm g_s / [(2l+1)g] \quad \text{for } I = l \pm \frac{1}{2}, \end{aligned} \quad (21)$$

and

$$\alpha_l = 1 - \alpha_s.$$

In order to reconcile the SP model on which (21) is based with the experimental magnetic moment, we postulate that the g_s of the odd proton in the nucleus is not that of a free proton but has an effective value, $g_s(\text{eff})$ chosen in such a way as to make (20) predict the observed magnetic moment. Such a procedure has been proposed by Bloch,⁴² de-Shalit,⁴³ and Miyazawa⁴⁴ and can be justified physically by the effect of meson exchange currents in the nucleus.

Proceeding with this scheme, we calculate an effective value of g_s by equating the right side of (20) to μ_{exp} and using it in (21). We find

$$\begin{aligned} \text{Sb}^{121}: \quad \alpha_s &= 0.405, \quad \alpha_l = 0.595, \\ \text{Sb}^{123}: \quad \alpha_s &= -0.535, \quad \alpha_l = 1.535. \end{aligned} \quad (22)$$

The value of $\langle R^2/R_0^2 \rangle_{Av}$ depends on the orbital angular momentum of the odd nucleon and Bohr^{37,45} calculates

TABLE III. Comparison of the experimental and theoretical values of the nuclear moments and hfs anomaly of Sb¹²¹ and Sb¹²³. The models used are described in the text.

Model	Sb ¹²¹		Sb ¹²³		Δ (%) ^a
	μ (nm)	ϵ^{BW} (%)	μ (nm)	ϵ^{BW} (%)	
SP	4.8 ^b	-0.63	1.7 ^b	-0.30	-0.34
C	3.75 ^c	-0.65	2.3 ^{c,d}	-0.36	-0.30
SU	...	-0.80	...	-0.08	-0.73
CM	3.54 ^e	-0.54	2.47 ^e	-0.17	-0.37
Exptl.	3.36	...	2.55	...	-0.352 ± 0.005

^a $\Delta = \Delta^{\text{BW}} + \Delta^{\text{RB}}$.

^b μ is the strict SP value but ϵ_{SP} is calculated by using $g_s(\text{eff})$ (see text).

^c Strong-coupling case—see A. Bohr and B. R. Mottelson, Kgl. Danske Videnskab. Selskab, Mat.-fys. Medd. 27, 16 (1953).

^d Some $g_{3/2}$ admixture—see (c).

^e See reference (53) and Sec. E(c) IV of this paper.

⁴¹ T. Schmidt, Z. Physik 106, 358 (1939).

⁴² F. Bloch, Phys. Rev. 83, 839 (1951).

⁴³ A. de-Shalit, Helv. Phys. Acta 24, 296 (1951).

⁴⁴ H. Miyazawa, Progr. Theoret. Phys. (Japan) 6, 263 (1951).

⁴⁵ A. Bohr (private communication quoted in reference 6).

$\langle R^2/R_0^2 \rangle_{Av} \approx 0.66$ and 0.90 for protons in d and g orbits, respectively. For the SP model,³⁷

$$\begin{aligned} \zeta &= (2I-1)/4(I+1), \quad (I = l + \frac{1}{2}) \\ \zeta &= (2I+3)/4I, \quad (I = l - \frac{1}{2}). \end{aligned} \quad (23)$$

We are now in a position to calculate ϵ_{SP} , and find

$$\epsilon_{\text{SP}}(\text{Sb}^{121}) = -0.625\% \quad \text{and} \quad \epsilon_{\text{SP}}(\text{Sb}^{123}) = -0.295\%$$

so that $\Delta_{\text{SP}}^{\text{BW}} = -0.33\%$.

II. Collective Model (C)

Bohr has suggested a modified single-particle model in which the odd particle is coupled to a rotating asymmetric core. This model has been very successful not only in predicting moments but also in explaining quadrupole moments and rotational excited states of heavy nuclei.^{36,37}

Several limiting cases of the collective model have been discussed by Bohr.³⁷ They differ principally in the strength of the assumed spin-orbit coupling compared with the coupling of the odd nucleon to an axis of the nucleus and the rotational level spacing of the nucleus.

We shall here consider only the case of intermediate coupling. The coupling parameter β depends on the strength of the $l-s$ coupling relative to the coupling between the orbit of the odd nucleon to the nuclear symmetry axis. Its value is chosen in such a way as to make the predicted value of the nuclear moment agree with experiment.

β is related to σ , the average value of the odd-particle spin component, by

$$\beta^2 = (1 - 2\sigma) / (1 + 2\sigma), \quad (24)$$

the positive root applying to $I = l + s$ and the negative sign to the case $I = l - s$. The quantity σ is given by

$$\sigma = \frac{(I+1)g_I - g_R - Ig_l}{g_s - g_l}, \quad (25)$$

where g_R is the g factor for nuclear rotation which is of the order of Z/A . The quantities α_s and α_l are given by

$$\alpha_s = \sigma g_s / (I+1)g_I, \quad \alpha_l = 1 - \alpha_s. \quad (26)$$

From (24), (25), and (26), we find that

$$\begin{aligned} \text{Sb}^{121}: \quad \alpha_s &= 0.445, \quad \alpha_l = 0.555, \\ \text{Sb}^{123}: \quad \alpha_s &= -0.243, \quad \alpha_l = 1.243. \end{aligned} \quad (27)$$

The asymmetry factor ζ is given by³⁸

$$\begin{aligned} \zeta &= \frac{2I-1}{4(I+1)}; \quad I = l + s, \\ \zeta &= \frac{1}{4(I+2)} \frac{1}{\beta^2 - 1} \\ &\times [\beta^2(2I+1) - 6\beta(2I+1)^{\frac{1}{2}} + 5 - 2I]; \quad I = l - s. \end{aligned} \quad (28)$$

Using the values of $\langle R^2/R_0^2 \rangle_{Av}$ and b given above and α_s , α_l , and ζ in (19), we find for the collective model

$$\epsilon_C(\text{Sb}^{121}) = -0.652\%, \quad \epsilon_C(\text{Sb}^{123}) = -0.363\%, \\ \Delta_C^{\text{BW}} = -0.29\%.$$

III. Single Particle—Uniform Interpolation Model⁴⁶ (SU)

Trigg,⁴⁷ Davidson,^{48,49} and Feenberg^{49,50} have described a nuclear model which combines features of both the single-particle and the uniform model of the nucleus.

The uniform model developed by Margenau and Wigner⁵¹ distributes the orbital angular momentum more or less at random over all the nucleons so that $g_l = Z/A$ for both protons and neutrons. The value of g_s is the same as in the SP model, 5.585 for protons and -3.83 for neutrons. The magnetic moment according to the uniform model is given by Eq. (20) with these values of g_s and g_l .

In the single particle—uniform interpolation model (SU) the empirical value of the magnetic moment is explained by postulating a mixture between the SP wave function for the nearest Schmidt assignment ($I = l \pm \frac{1}{2}$) and the many-particle wave function corresponding to the opposite Margenau-Wigner limit ($I = l \mp \frac{1}{2}$). The quantity l is the appropriate orbital quantum number to give the same I to both states. (It is not permissible to mix the SP states corresponding to $I = l \pm \frac{1}{2}$ since they have opposite parity.) Calling the fractional SP admixture f , we have

$$g_{\text{SU}} = f g_{\text{SP}} + (1-f) g_{\text{U}}, \quad (29)$$

where g_{SP} and g_{U} are those of the nearest Schmidt line and the opposite Margenau-Wigner limit, respectively. The parameter f is chosen by setting g_{SU} equal to g_{exp} in (29) and the hfs anomaly is found from

$$\epsilon_{\text{SU}} = f \epsilon_{\text{SP}} + (1-f) \epsilon_{\text{U}}. \quad (30)$$

For Sb^{121} and Sb^{123} , g_{SP} is calculated for the odd proton in the $d_{5/2}$ and $g_{7/2}$ states, respectively. These assignments corresponding to the nearest lying Schmidt lines. On the other hand, g_{U} is determined for the $f_{5/2}$ and $f_{7/2}$ proton states. In this way we find the following values of f from (14):

$$f(\text{Sb}^{121}) = 0.74 \quad \text{and} \quad f(\text{Sb}^{123}) = 0.65.$$

⁴⁶ This empirical model has had some success in predicting magnetic moments but has little physical basis. It is included in the present discussion mainly to illustrate the sensitivity of the calculation of Δ on the model assumed.

⁴⁷ G. L. Trigg, Phys. Rev. **86**, 506 (1952).

⁴⁸ J. P. Davidson, Phys. Rev. **85**, 432 (1952).

⁴⁹ J. P. Davidson and E. Feenberg, Phys. Rev. **89**, 856 (1953).

⁵⁰ E. Feenberg, *Shell Theory of the Nucleus* (Princeton University Press, Princeton, 1955), p. 36.

⁵¹ H. Margenau and E. P. Wigner, Phys. Rev. **58**, 103 (1940).

To calculate ϵ_{U} , we recall that the uniform model has no angular symmetry so that $\zeta = 0$. $\langle R^2/R_0^2 \rangle_{Av}$ is that of a uniformly charged sphere, i.e., $\frac{3}{5}$, so that from (18)

$$\epsilon_{\text{U}} = -\frac{3}{5}(\alpha_s + 0.62\alpha_l)b, \quad (31)$$

with

$$\alpha_s = \pm g_s / (2l+1)g_{\text{U}}. \quad (32)$$

ϵ_{SP} is found from (19), (22), and (23) using $g_s = 5.585$ and $g_l = 1$.

Substituting these values for ϵ_{U} and ϵ_{SP} in (30), we finally obtain

$$\epsilon_{\text{SU}}(\text{Sb}^{121}) = -0.80\%, \quad \epsilon_{\text{SU}}(\text{Sb}^{123}) = -0.08\%$$

and

$$\Delta_{\text{SU}}^{\text{BW}} = -0.72\%.$$

IV. Configuration Mixing Model (CM)

Recently Arima and Horie⁵² and Blin-Stoyle and Perks⁵³ have suggested a model which is remarkably successful in predicting many nuclear moments. The model is again based on the SP model, the deviations of μ_{exp} from the Schmidt values being explained by small amplitudes of non-ground-state configurations being mixed in with the SP states.

The configuration mixing coefficient is determined from general considerations such as the energy level spacings between unperturbed ground state and excited configurations, and estimates of the nuclear pairing energy. It is a remarkable fact that even quite large deviations from the Schmidt lines can be explained by mixing coefficients of the order of 0.1. Only configurations whose spin differs from the SP configuration spin by unity and which have the same orbital quantum number need to be considered. Without any other adjustable parameters μ_{CM} is calculated from formulas derived in the Appendix of reference 52. The results for Sb^{121} and Sb^{123} are given in Table III. They are based on the proton and neutron configurations given below which are somewhat different from those which were used by Arima and Horie in their calculations. Only those proton and neutron states for which configuration mixing is possible and contributes to the deviation of μ from the SP value are listed.

$$\text{Sb}^{121}; \quad p: (g_{9/2})^{10}, \quad n: (d_{5/2})^6 (h_{11/2})^4,$$

$$\text{Sb}^{123}; \quad p: g_{7/2}, \quad n: (d_{5/2})^6 (h_{11/2})^6.$$

The contribution to μ_{CM} of μ_{SP} as well as of each of the possible proton and neutron excitations (μ_{exc}) are calculated according to the formulas in reference 52 and the values of ϵ are determined for each of them according to (19), using appropriate values of $\langle R^2/R_0^2 \rangle_{Av}$. The various ϵ 's are weighted according to the contribution

⁵² A. Arima and H. Horie, Progr. Theoret. Phys. (Japan) **12**, 623 (1954).

⁵³ R. J. Blin-Stoyle and M. A. Perks, Proc. Phys. Soc. (London) **A67**, 855 (1954).

μ_{SP} or μ_{exc} makes to μ_{CM} . The final results⁵⁴ are

$$\epsilon_{CM}(Sb^{121}) = -0.538\%, \quad \epsilon_{CM}(Sb^{123}) = -0.173\%, \\ \Delta_{CM}^{BW} = -0.365\%.$$

(e) Discussion of Nuclear Models

In the preceding section we have considered four plausible nuclear models for Sb¹²¹ and Sb¹²³ which attempt to reconcile empirical values of the magnetic moment with the Schmidt value. In the SP model this is done by postulating a $g_s(\text{eff})$ which is different from that of the free nucleon. The collective model (C) postulates strong coupling of the odd particle to the nuclear core, while the CM model mixes excited configurations to the ground state configuration. The SU model, finally, is a compromise between a strict SP model and a uniform model in which the orbital angular momentum is shared. The values of ϵ^{BW} obtained from these models are collected in Table III along with predicted values of the nuclear moments.

If we use a comparison between theoretical and

⁵⁴ We are indebted to Dr. V. Jaccarino and Dr. H. Stroke for illuminating discussions on the calculation of Δ_{CM}^{BW} . [See also H. Stroke and V. Jaccarino, *Bull. Am. Phys. Soc. Ser. II*, **2**, 228 (1957)].

experimental values of Δ as a criterion for the quality of the models, we can eliminate only the SU model. All others give reasonably good agreement (see Table I). In the final analysis we must therefore fall back on more general considerations in trying to evaluate these models like predictions of quadrupole moments and excited rotational states⁵⁵ which favor the collective model.

In conclusion we might say that our results seem to justify the generally accepted nuclear models without being very sensitive to variation in details of these models. The methods used in this experiment to measure the hfs anomaly are new and should be fruitful in bringing several other nuclei under experimental scrutiny.

F. ACKNOWLEDGMENTS

We wish to thank Dr. V. Jaccarino, Dr. W. Kohn, and Dr. A. L. Schawlow for many stimulating and helpful discussions on this problem, Dr. R. G. Shulman for discussions and collaboration in the measurement of the antimony moments, Mr. E. A. Gere for his assistance in the experiment, and Miss C. L. Monahan for help in the computations.

⁵⁵ A. Bohr and B. R. Mottelson, *Kgl. Danske Videnskab. Selskab, Mat.-fys. Medd.* **27**, 16 (1953).

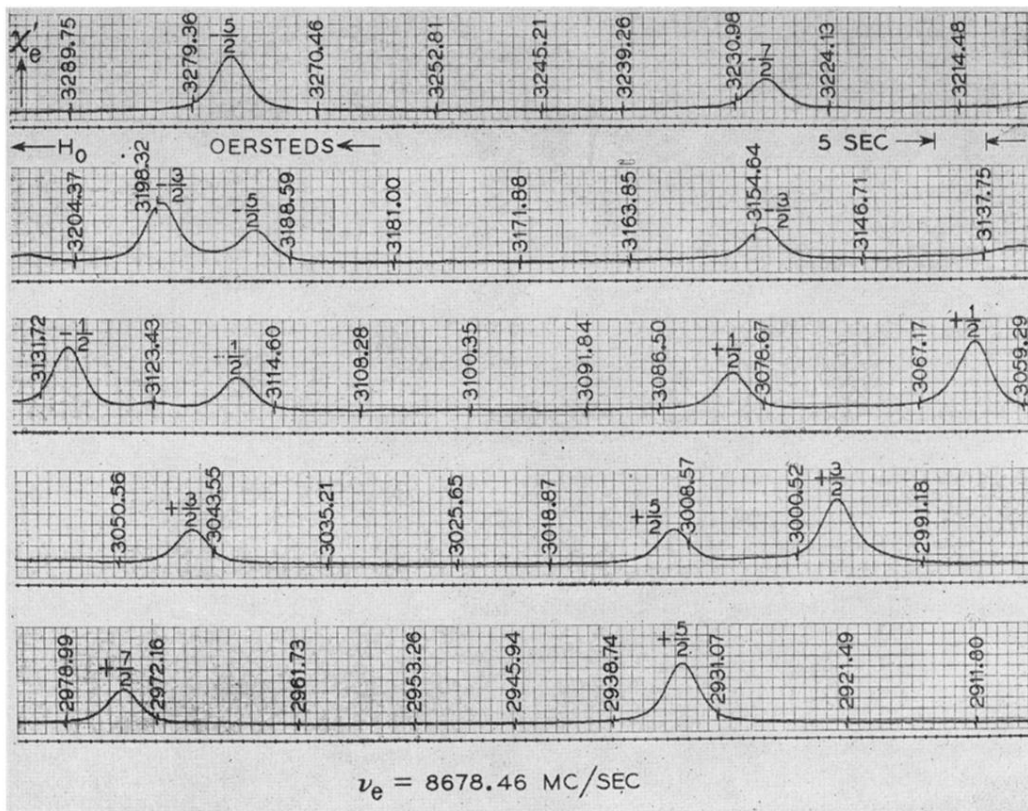


FIG. 2. Experimentally observed spectrum of the microwave transitions for Sb¹²¹ and Sb¹²³.
 The field markers are derived from a proton resonance.

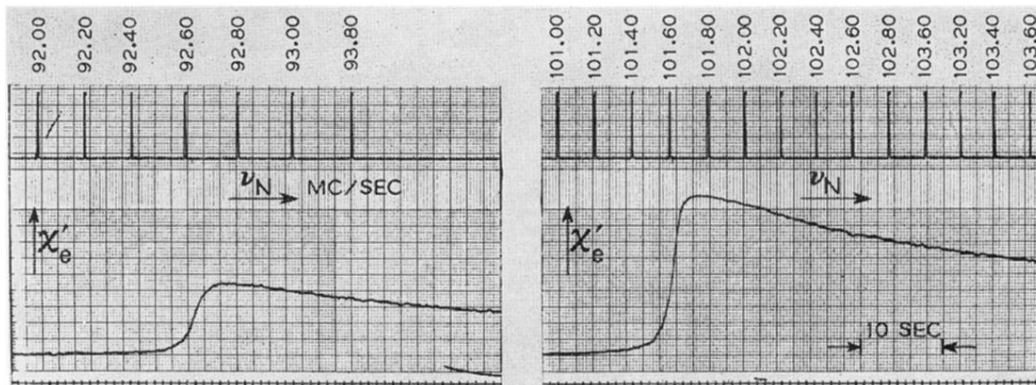


FIG. 3. Observation of the hyperfine transitions via the electron spin resonance line (ENDOR technique). The ratio of amplitudes is explained in Fig. 4. The asymmetry is caused by the long spin-lattice relaxation time [see Sec. C(d)].